• Basic Research •

Screening for differentially expressed genes in retinoblastoma gene chips through the GEO database and validation in clinical settings

Chun-Yi Liu[1,2], Rui Luo[1,2], Han Liu[1,2], Ruo-Yi Xie[1], Yong Chai[1,2], Yu Xu[3]

[1]Department of Ophthalmology, Jiangxi Provincial Children's Hospital, The Affiliated Children's Hospital of Nanchang Medical College, Nanchang 330006, Jiangxi Province, China
[2]The Affiliated Eye Hospital, Jiangxi Medical College, Nanchang University, Nanchang 330006, Jiangxi Province, China
[3]Department of Ophthalmology, Xinhua Hospital Affiliated to Shanghai Jiao Tong University School of Medicine, Shanghai 200000, China
Co-first Authors: Chun-Yi Liu and Rui Luo
Correspondence to: Yong Chai. Jiangxi Provincial Children's Hospital & The Affiliated Eye Hospital, Jiangxi Medical College, Nanchang University, Nanchang 330006, Jiangxi Province, China. cyjxsetyy@126.com; Yu Xu. Xinhua Hospital Affiliated to Shanghai Jiao Tong University School of Medicine, Shanghai 200000, China. xuyu01@xinhuamed.com.cn
Received: 2025-04-02 Accepted: 2026-02-04

Abstract

● **AIM:** To screen for differentially expressed genes in retinoblastoma (RB) gene chips using GEO2R and validate them clinically.

● **METHODS:** The expression profile chip data (GSE110811) was downloaded from the public gene chip database Gene Expression Omnibus (GEO). The GEO2R chip analysis platform was used to identify differentially expressed genes between RB and adjacent normal tissues. According to the International Intraocular Retinoblastoma Classification (IIRC) system, 35 children diagnosed with RB from our hospital and other hospitals were enrolled as the RB group, and 35 healthy children who underwent physical examinations in our hospital were enrolled as the control group. The relative expression levels of Sprouty RTK signaling antagonist 2 (SPRY2) and estrogen-related receptor beta (ESRRB) in the serum of patients were detected by quantitative reverse transcription polymerase chain reaction (qRT-PCR). The diagnostic value of SPRY2 and ESRRB in RB was evaluated by receiver operating characteristic (ROC) curves. Analysis of the relationship between SPRY2/ESRRB expression and clinicopathological features, as well as its correlation with the tumor marker CA199.

● **RESULTS:** In the GSE110811 chip, the expression levels of two genes, 16780069 (SPRY2) and 16786783 (ESRRB), showed the most significant differences between RB and normal tissues. The relative expression levels of SPRY2 and ESRRB in the serum of children in RB group (22 males, age 1.64±1.08y) were significantly lower (P<0.05) than those in control group (25 males, age 1.54±0.95y). The area under the ROC curve for SPRY2 was 0.735 (95%CI: 0.616-0.854), while that for ESRRB was 0.880 (95%CI: 0.800-0.960). There were statistically significant differences in the expression of SPRY2 and ESRRB with respect to choroidal invasion, optic nerve invasion, differentiation degree, and clinical staging (P<0.05). In RB group, the expression levels of SPRY2 and ESRRB decreased gradually with increasing CA199 levels, showing a negative correlation (r_{SPRY2}=-0.593, r_{ESRRB}=-0.423; both P<0.05).

● **CONCLUSION:** The expression of SPRY2 and ESRRB is closely related to the occurrence and development of RB and negatively correlated with the tumor marker CA199. They have the potential to serve as diagnostic biomarkers for RB.

● **KEYWORDS:** GEO database; retinoblastoma; clinical validation

DOI:10.18240/ijo.2026.05.04

Citation: Liu CY, Luo R, Liu H, Xie RY, Chai Y, Xu Y. Screening for differentially expressed genes in retinoblastoma gene chips through the GEO database and validation in clinical settings. *Int J Ophthalmol* 2026;19(5):869-877

INTRODUCTION

Retinoblastoma (RB) is a highly malignant ocular tumor that predominantly occurs in infants and young children and is considered one of the most severe pediatric malignancies[1]. Studies have shown that RB accounts for 4% of all pediatric malignancies, and more than 5% of affected children become blind due to this disease[2]. The incidence of RB varies significantly between domestic and international

reports, but regardless of the differences, its detrimental impact on children's vision and overall health is undeniable[1]. Therefore, early detection and diagnosis are key factors in improving cure rates and reducing mortality in affected children. Due to the young age of the patients, children with RB often cannot accurately describe their symptoms. Additionally, the disease is relatively insidious in its onset, and most patients are diagnosed at an advanced stage[3]. For children with intermediate or advanced RB, current clinical treatments mainly involve enucleation or external beam radiotherapy. Although these treatments offer relatively good prognosis, the overall 5-year survival rate is still far from satisfactory compared to that of developed countries, where it ranges from 87% to 97%[4-5]. Research has demonstrated that early detection of RB is associated with more favorable clinical outcomes[6]. Therefore, the importance of early treatment, prevention, and diagnosis of RB cannot be overstated.

In recent years, with the continuous development and improvement of microarray technology, it has been widely applied and has generated a vast amount of biological information data, providing rich resources for life science research[7]. Due to the increase in data information, a variety of databases have emerged[8-9]. The Gene Expression Omnibus (GEO), a high-throughput gene expression database, is currently the largest public database and offers free services to the public[10]. In this study, we searched the GEO database for microarray data related to RB and identified differential expression of sprouty RTK signaling antagonist 2 (*SPRY2*) and estrogen-related receptor beta (*ESRRB*) in RB patients. *SPRY2* is a tumor suppressor gene in organisms and can inhibit important biological functions such as cell proliferation, invasion, and migration[11-12]. *ESRRB* encodes a protein similar to the estrogen receptor, and recent studies have shown that ESRRB acts as a negative regulator of the cell cycle and may function as a tumor suppressor gene, with the potential to become a therapeutic target[13]. However, no studies have yet explored the roles of these two genes in RB.

Therefore, this study aims to confirm the expression of SPRY2 and ESRRB in RB through GEO microarray screening combined with clinical experiments, and to explore their potential as diagnostic and prognostic indicators for RB, providing references for clinical practice.

PARTICIPANTS AND METHODS

Ethical Approval This study has been approved by the Jiangxi Provincial Children's Hospital Ethics Committee (Approval No.JXSETYY-YXKY-20240212). The parents of participants were informed of the purpose of the study and signed an informed consent form.

Retrieval of Retinoblastoma Data from National Center for Biotechnology Information Platform Log in to the National Center for Biotechnology Information platform (https://www.ncbi.nlm.nih.gov/). Change the option in the top-left corner from "All Databases" to "GEO Datasets". Enter "Retinoblastoma" in the search bar and click "Search" to retrieve the relevant data.

Screening of Differentially Expressed Genes Using GEO2R First, open the GEO2R microarray analysis platform (https://www.ncbi.nlm.nih.gov/geo/geo2r/). Enter the selected microarray code (GSE110811) in the GEO accession field. Then click on "Define groups" for sample grouping. We assigned 28 RB samples to RB group and 3 normal samples to normal group. Next, select "View" under Value distribution to analyze whether there is any bias in the data of the microarray. Once the data is confirmed to be complete and usable, select the "Top 250" option in GEO2R to obtain the top 250 genes ranked by the smallest to largest *P*-values of differential gene expression between the two groups.

Clinical Data of Patients A total of 35 RB patients who received treatment in our hospital and other hospitals from February 2016 to February 2018 were enrolled as the RB group in this study. Among them, there were 22 male patients and 13 female patients, with an average age of 1.64±1.08y. Additionally, 35 normal children who underwent physical examinations in our hospital were collected as the control group, including 25 males and 10 females, with an average age of 1.54±0.95y. The control group children had normal biochemical, blood routine, immune, and microbiological tests, and no congenital defects or diseases were present. According to the IIRC system, the stages were represented as A, B, C, D, and E. All children underwent ocular ultrasound (B-mode ultrasound or color Doppler ultrasound), computed tomography (CT)/magnetic resonance imaging (MRI), and fundus photography (Ret Cam infant fundus camera) to confirm the diagnosis of RB and could be staged according to the IIRC system. The clinical data of the children were complete.

Children with other tumors, congenital immune or systemic defects, severe trauma or infections, or those who had undergone prior treatment (such as radiotherapy or chemotherapy) were excluded.

Sample Collection Five milliliters of peripheral venous blood were collected from the children before treatment. The blood samples were allowed to stand for 30min, followed by centrifugation at 3500 rpm for 10min at 4℃. The supernatant was collected and stored at -80℃ for subsequent use.

PCR Amplification Total RNA was extracted from the serum using TRIzol reagent (Thermo Fisher Scientific, Shanghai, China, 12183555). The purity, concentration, and integrity of the extracted total RNA were assessed using a UV spectrophotometer and agarose gel electrophoresis.

Quantitative reverse transcription polymerase chain reaction (qRT-PCR) was performed using the TransScript II Green two-step qRT-PCR Super Mix (TransGen Biotech, Beijing, AQ301-01) according to the manufacturer's instructions. The PCR amplification system included: 1 μL of cDNA, 0.4 μL of each forward and reverse primer, 10 μL of 2× TransScript® Tip Green qPCR Super Mix, and passive reference dye (50×), with nuclease-free water added to a final volume of 20 μL. The PCR conditions were as follows: pre-denaturation at 94℃ for 30s, followed by 40 cycles of denaturation at 94℃ for 5s, and annealing and extension at 60℃ for 30s. The primers used were as follows: for SPRY2, forward primer 5'-ATCCAGAGCAAGACATG-3' and reverse primer 5'-TTCAGATGTGTTCTA-3'; for ESRRB, forward primer 5'-CCTGCTGAGGCAGACAGCCG-3' and reverse primer 5'-GGTTCTCCTCCACGTCGCCG-3'; for GAPDH, forward primer 5'-ACCACAGTCCATGCCATCAC-3' and reverse primer 5'-TCCACCACCCTGTTGCTGTA-3'. Each sample was run in triplicate, and the experiment was repeated three times. GAPDH was used as the internal reference gene, and the data were analyzed using the $2^{-\Delta\Delta ct}$ method. The process was performed using the ABI 7500 Real-Time PCR System (Applied Biosystems, USA).

Detection of CA199 The expression levels of CA199 in the collected serum samples from the pediatric patients were measured using a fully automated chemiluminescent immunoassay analyzer (Roche, USA; model: Cobase601). The detection protocol was performed according to the manufacturer's instructions, with a reference range for CA199 defined as <39.00 kU/L. Although CA199 is not a standard marker for RB, Liu *et al*[14] reported that it was significantly elevated in the serum of RB patients and was associated with tumor burden. This study verified its negative correlation with SPRY2/ESRRB and aimed to explore the potential of new marker combinations.

Treatment Protocol for Patients The 35 children were treated according to their staging under the IIRC system. Children in stage A received local therapy, primarily laser photocoagulation and cryotherapy. Those in stages B and C were treated with chemotherapy. Children in stages D and E underwent enucleation surgery followed by adjuvant chemotherapy. The chemotherapy regimen consisted of a combination of carboplatin, etoposide, and vincristine, as follows: vincristine 1.5 mg/m^2 administered as a slow intravenous injection once weekly for 3wk; etoposide 150 mg/m^2 given as a 1-hour intravenous injection once daily for 3d (days 1–3); and carboplatin 560 mg/m^2 administered as a 1-hour intravenous injection on day 1 of the chemotherapy cycle, for a single day. One treatment cycle lasted 3wk, and a total of 3 to 6wk were administered.

Statistical Analysis SPSS 20.0 software was used to analyze the collected data, and GraphPad Prism 7 software was employed to generate relevant figures. The distribution of the data was analyzed using the Kolmogorov-Smirnov (K-S) test. Categorical data were presented as percentages (%) and analyzed using the Chi-square test, denoted as χ^2. Ordinal data were analyzed using non-parametric tests. Continuous data were expressed as mean±standard deviation (SD). Normally distributed data were analyzed using the *t*-test, with independent samples *t*-test used for between-group comparisons. Non-normally distributed data were analyzed using the rank-sum test. Comparisons among multiple groups were performed using one-way analysis of variance, with post-hoc analysis conducted using the LSD-t test. The diagnostic value of the two genes in RB was assessed using receiver operating characteristic (ROC) curve analysis. Pearson correlation analysis was used to evaluate the relationships between SPRY2, ESRRB, and CA199. A significance threshold of $P<0.05$ was considered statistically significant.

RESULTS

Basic Information of the Chip After retrieving the chip through the retrieval process, the GSE110811 gene chip was ultimately selected. The basic information of this chip is shown in Table 1.

Bias of Chip Data Through the value distribution function in GEO2R, it was found that the data in the GSE110811 chip did not show significant bias errors and had good research value, as shown in Figure 1.

Differentially Expressed Genes Screening Results Through the analysis of GEO2R, it was found that in the GSE110811 chip, the expression levels of the two genes with gene IDs 16780069 and 16786783 showed the most significant differences between RB and normal, with both being lowly expressed in the cancer (Figures 2 and 3). Moreover, their adjusted *P* value was the same (*P*=7.95e-10, 9.66e-10; adjusted *P*=0.0000128). These two genes attracted our attention. Subsequently, we checked their corresponding GB_ACC. The GB_ACC of gene 16780069 was NM_005842, and that of gene 16786783 was NM_004452. After searching through the Gene option in NCBI, we found that these two gene IDs corresponded to SPRY2 and ESRRB, respectively. Therefore, we carried out further research on these two genes. The GSE110811 dataset has a small number of normal samples (*n*=3), which may affect the efficiency of differential gene screening. This study verified the reliability of the results by expanding the clinical sample size (*n*=70).

Analysis of Patient Clinical Data Comparison of the clinical data of the two groups of children showed that there were no statistical differences in gender, age, height, weight, maternal childbirth conditions, and place of residence between the control group and the RB group ($P>0.05$), as shown in Table 2.

Table 1 Basic information of the GSE110811 chip

Data	GSE110811
Time	
Submission date	Feb 19, 2018
Last update date	Jan 23, 2019
Contact name	Hans E. Grossniklaus
Address	
Organization name	Emory Eye Center
Street address	1365 Clifton Rd
City	Atlanta
State/Province	Georgia
Country	USA
ZIP/Postal code	30322
Organism	Homo sapiens
Experiment type	Expression profiling by array
Platforms	GPL16686 [HuGene-2_0-st] Affymetrix Human Gene 2.0 ST Array [transcript (gene) version]
Sample number (used/total)	31/34

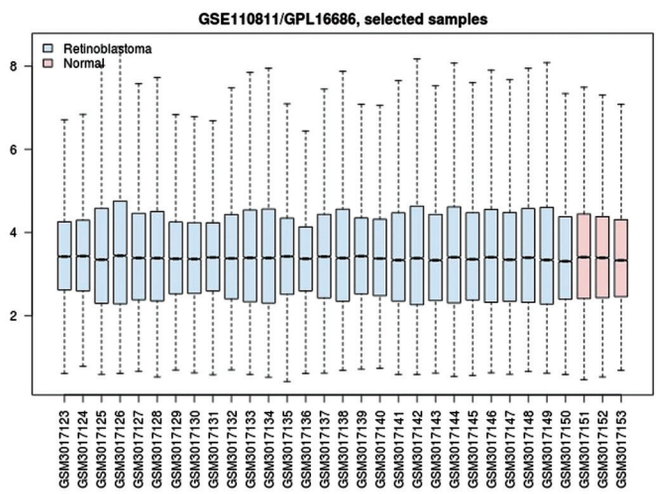

Figure 1 Bias of data in GSE110811 chip The data between retinoblastoma and normal have good comparability and no significant bias errors.

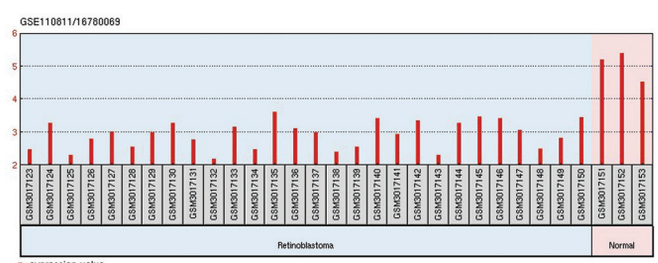

Figure 2 Expression of gene 16780069 (SPRY2) in the chip The expression of gene is much higher in normal individuals than in retinoblastoma patients. SPRY2: Sprouty RTK signaling antagonist 2.

Expression of SPRY2 and ESRRB in the Serum of Children in the Two Groups Detection of the expression in the serum of the two groups of patients revealed that the relative expression of SPRY2 and ESRRB in the serum of children in the RB group was significantly lower than that of children in the control group, with significant differences (t_{SPRY2}=3.532, P=0.001; t_{ESRRB}=6.387, P<0.001), as shown in Figure 4.

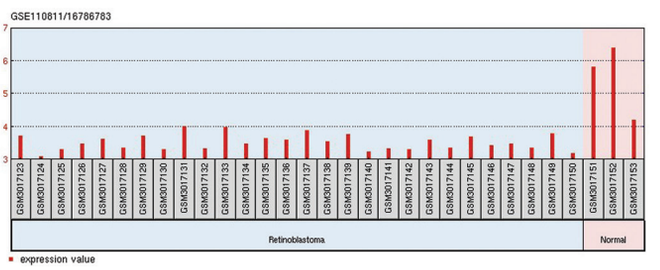

Figure 3 Expression of gene 16786783 (ESRRB) in the chip The expression of gene is much higher in normal individuals than in retinoblastoma patients. ESRRB: Estrogen-related receptor beta.

Diagnostic Value of SPRY2 and ESRRB in Normal Children and Children with Retinoblastoma Based on the expression of SPRY2 and ESRRB in the serum of children in the two groups, the ROC curve was drawn. It was found that the area under the curve (AUC) of SPRY2 was 0.735, with a 95% confidence interval (CI) of 0.616–0.854. The AUC of ESRRB was 0.880, with a 95%CI of 0.800–0.960, indicating a higher diagnostic value (Figure 5 and Table 3).

Relationship Between SPRY2, ESRRB and Pathological Data in Children with Retinoblastoma Analysis based on the clinical pathological data of children revealed that there were no statistical differences between SPRY2 and ESRRB and the gender, age, maternal childbirth conditions, and affected eye of the children (P>0.05). However, there were statistical differences with regard to choroidal invasion, optic nerve invasion, degree of differentiation, and clinical staging (P<0.05), as shown in Table 4.

Relationship Between SPRY2, ESRRB and CA199 Comparison of the correlation between the relative expression of SPRY2 and ESRRB and CA199 in children in the RB group revealed that the expression of SPRY2 and ESRRB in children in the RB group gradually decreased with the increase

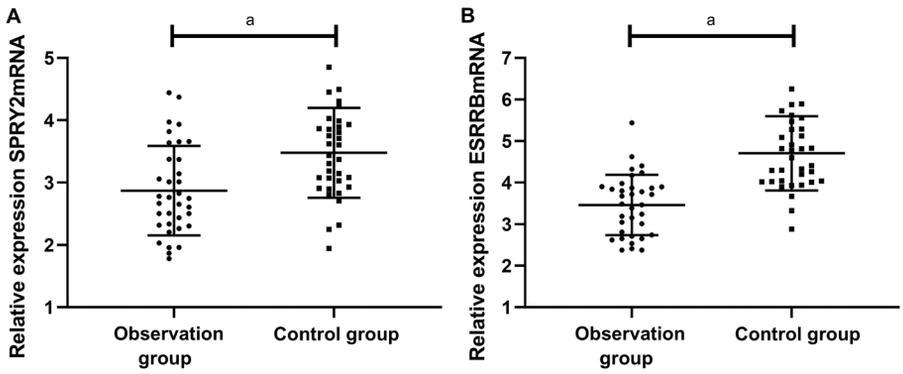

Figure 4 Expression of SPRY2 and ESRRB in the serum of children A: Expression of SPRY2 in the serum of children in the RB group (2.871±0.717) and the control group (3.478±0.719); B: Expression of ESRRB in the serum of children in RB group (3.462±0.726) and control group (4.705±0.894). ^{a}P<0.001. RB: Retinoblastoma; SPRY2: Sprouty RTK signaling antagonist 2; ESRRB: Estrogen-related receptor beta.

Table 2 Characteristics of two groups *n* (%) or mean±SD

Factors	Control group (*n*=35)	RB group (*n*=35)	t/χ^2	*P*
Gender			0.583	0.445
Male	25 (71.43)	22 (62.86)		
Female	10 (28.57)	13 (37.14)		
Age (y)	1.54±0.95	1.64±1.08	0.411	0.682
Height (cm)	88.51±4.25	89.17±5.74	0.547	0.586
Weight (kg)	12.35±2.12	13.11±2.41	1.401	0.166
Maternal childbirth conditions			0.229	0.584
Primipara	25 (71.43)	27 (77.14)		
Multipara	10 (28.57)	8 (22.86)		
Place of residence			0.265	0.607
Rural	12 (34.29)	10 (28.57)		
Urban	23 (65.71)	25 (71.43)		
Affected eye				
Unilateral	-	22 (62.86)		
Bilateral	-	13 (37.14)		
Choroidal invasion				
Yes	-	10 (28.57)		
No	-	25 (71.43)		
Optic nerve invasion				
Yes	-	13 (37.14)		
No	-	22 (62.86)		
Degree of differentiation				
Differentiated	-	17 (48.57)		
Undifferentiated	-	18 (51.43)		
IIRC staging				
Stage A	-	5 (14.29)		
Stage B	-	4 (11.43)		
Stage C	-	3 (8.57)		
Stage D	-	13 (37.14)		
Stage E	-	10 (28.57)		
CA199 (kU/L)	19.84±12.22	41.62±18.77		

RB: Retinoblastoma; IIRC: International Intraocular Retinoblastoma Classification; CA199: Carbohydrate antigen 19-9.

of CA199, and there was a negative correlation between the groups (Figure 6).

DISCUSSION

RB is a common primary intraocular tumor in children. In China, the diagnosis rate of RB in children is only 63%[15]. Although great progress has been made in the treatment and prognosis of RB in recent years with the improvement of medical standards, the mortality and recurrence rates of RB are still high worldwide, and the survival rate in developing countries is significantly lower than that in developed countries[16-18]. Studies have shown[19] that 6% of cases are autosomal dominant inheritance, and 94% of patients have sporadic pathology, among which 25% of patients have hereditary mutations, and the rest are somatic mutations. Other

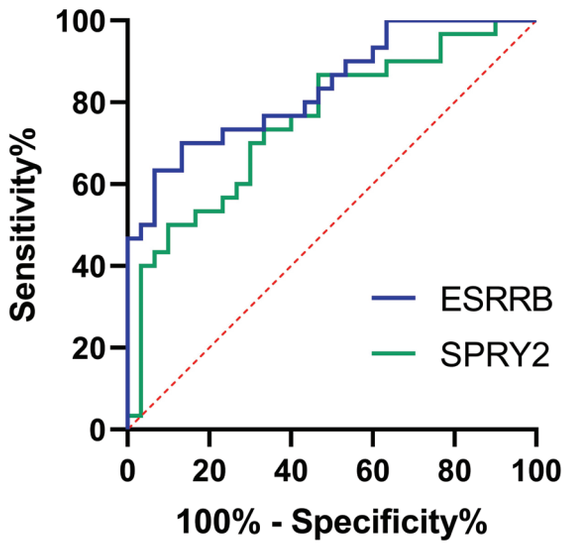

Figure 5 Diagnostic value of SPRY2 and ESRRB in retinoblastoma SPRY2: Sprouty RTK signaling antagonist 2; ESRRB: Estrogen-related receptor beta.

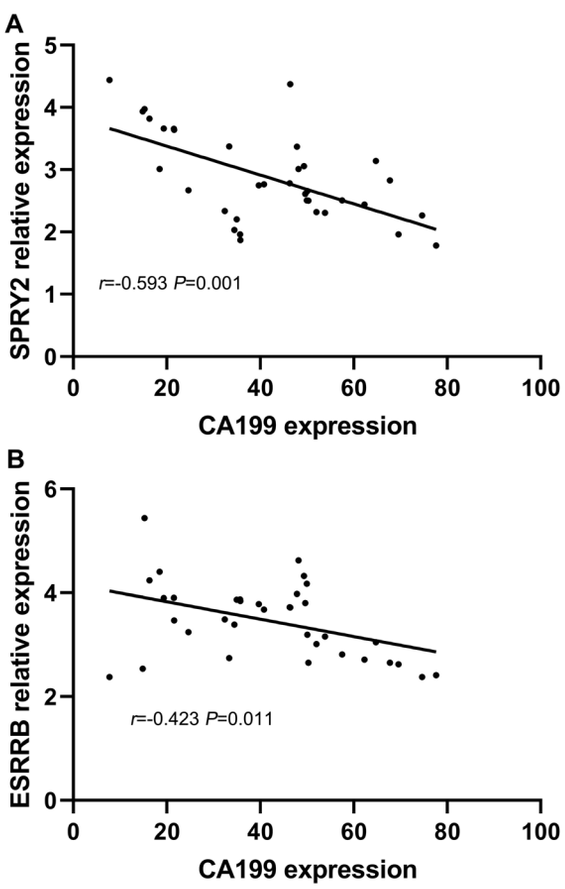

Figure 6 Correlation analysis between SPRY2, ESRRB and CA199 A: SPRY2 expression is negatively correlated with CA199 expression (r=-0.593, P=0.001); B: ESRRB expression is negatively correlated with CA199 expression (r=-0.423, P=0.011). SPRY2: Sprouty RTK signaling antagonist 2; ESRRB: Estrogen-related receptor beta; CA199: Carbohydrate antigen 19-9.

literature indicates[20] that after the occurrence of RB, there will be differential expression of genes and proteins. Therefore, whether it is possible to use the differential expression of genes and proteins in patients as a potential indicator for the occurrence of RB is a new way for clinical researchers to find treatments and diagnose RB.

Table 3 ROC parameters

Factors	SPRY2	ESRRB
AUC	0.735	0.880
95%CI	0.616–0.854	0.800–0.960
SE	0.061	0.041
Specificity	57.14%	80.00%
Sensitivity	88.57%	88.57%
Youden Index	45.71%	68.57%
Cutoff	>2.795	>3.915

ROC: Receiver operating characteristic; SPRY2: Sprouty RTK signaling antagonist 2; ESRRB: Estrogen-related receptor beta; AUC: Area under the curve; CI: Confidence interval; SE: Standard error; Cutoff: Optimal cutoff point.

With the continuous upgrading of microarray technology, it has been widely used. High-throughput sequencing technology, also known as "second-generation sequencing technology", involves sequencing hundreds of thousands or even millions of DNA molecules[21]. The TCGA and GEO, as the world's largest public resource databases, can provide high-throughput data analysis for a variety of diseases[22-23]. Therefore, in this study, we searched and screened the differentially expressed genes of RB through the GEO database to find potential diagnostic and prognostic indicators for RB. We first selected the GSE110811 chip for screening through the GEO database, and the results showed that the differences in *SPRY2* and *ESRRB* were the most significant, with both genes being lowly expressed in cancer patients. The release of circulating nucleic acids (cell-free RNA, cfRNA) by tumor tissue is the theoretical core of liquid biopsy. Its mechanism mainly stems from the apoptosis, necrosis or active secretion of tumor cells (such as exosomes), which allows the RNA (including mRNA) inside them to enter the blood circulation[24-25]. Recent studies have shown that the tumor microenvironment of RB also has this characteristic, and the exosomes secreted by it can carry specific tumor-derived mRNA into the blood[26]. This study shows that in RB, the expression changes of tissue differentially expressed genes *SPRY2* and *ESRRB* in serum are consistent with the tissue source, which provides an important theoretical basis and feasibility support for using the two as plasma markers for non-invasive diagnosis.

SPRY2 is a member of the signal pathway inhibitory protein family, and its structure contains a highly conserved C-terminal rich in cysteine[27]. Previous studies by Lao *et al*[28] have shown that SPRY2 has a more significant inhibitory effect on the RTK signaling pathway compared with the other three subtypes (SPRY1, 3, 4). ESRRB, as a member of the nuclear hormone receptor superfamily, has been shown[29] to be of

Table 4 Relationship between pathological data of children and SPRY2, ESRRB

Factors	SPRY2	ESRRB
Gender		
Male (*n*=22)	2.930±0.825	3.387±0.724
Female (*n*=13)	2.772±0.499	3.588±0.739
t	0.624	0.788
P	0.537	0.437
Age (y)		
≥2 (*n*=15)	2.761±0.723	3.441±0.825
<2 (*n*=20)	2.907±0.734	3.458±0.653
t	0.947	0.068
P	0.350	0.946
Maternal childbirth conditions		
Primipara (*n*=25)	3.243±0.805	3.666±0.578
Multipara (*n*=10)	3.380±0.772	3.480±0.772
t	0.469	0.686
P	0.642	0.497
Affected eye		
Unilateral (*n*=22)	2.954±0.625	3.625±0.795
Bilateral (*n*=13)	2.841±0.584	3.484±0.658
T	0.529	0.539
P	0.600	0.594
Choroidal invasion		
Yes (*n*=10)	2.625±0.725	2.789±0.699
No (*n*=25)	3.345±0.455	3.841±0.821
t	3.549	3.561
P	0.001	0.001
Optic nerve invasion		
Yes (*n*=13)	2.715±0.478	2.925±0.725
No (*n*=22)	3.511±0.594	3.955±0.844
t	4.103	3.668
P	<0.001	0.001
Degree of differentiation		
Differentiated (*n*=17)	2.524±0.418	2.795±0.725
Undifferentiated (*n*=18)	3.335±0.765	3.869±0.894
t	3.859	3.890
P	0.001	0.001
Clinical staging		
Stage A (*n*=5)	4.518±0.562	4.012±0.387[a]
Stage B (*n*=4)	3.586±0.490[a]	2.942±0.510[a]
Stage C (*n*=3)	3.217±0.532[a]	2.593±0.576[a]
Stage D (*n*=13)	3.150±0.573[a]	2.585±0.433[a]
Stage E (*n*=10)	2.388±0.020[a,b,c,d]	1.972±0.257[a,b,c,d]
F	18.362	21.909
P	<0.001	<0.001

[a]*P*<0.05 compared with Stage A; [b]*P*<0.05 compared with Stage B; [c]*P*<0.05 compared with Stage C; [d]*P*<0.05 compared with Stage D. SPRY2: Sprouty RTK signaling antagonist 2; ESRRB: Estrogen-related receptor beta.

great value in mouse embryonic development, and its absence can cause placental death. Research by Mustafi *et al*[30] has shown that ESRRB is highly expressed in the retina. In this study, we detected the expression of SPRY2 and ESRRB in the serum of children with RB through qRT-PCR and found that the expression of SPRY2 and ESRRB in the serum of children in the RB group was significantly lower than that of the control group, which was consistent with the results of the gene chip screening we conducted earlier. This indicates that SPRY2 and ESRRB have the potential to become biological indicators for distinguishing between children with RB and normal children. Although Mao *et al*[24] reported that SPRY2/ESRRB was downregulated in RB tissue, this study revealed the diagnostic value of both in serum (AUC=0.880), significant correlation with clinical stage and invasiveness (Table 4), and a negative correlation with CA199 (Figure 6). This provides a new perspective for non-invasive diagnosis. Therefore, we further drew the ROC curve of the expression of SPRY2 and ESRRB in children with RB and normal children and found that SPRY2 and ESRRB have good diagnostic value in RB, with AUC of 0.735 and 0.880, respectively. This suggests that detecting the expression of SPRY2 and ESRRB in the serum of children with RB can serve as a potential diagnostic indicator for RB. Subsequently, we further analyzed the relationship between SPRY2, ESRRB and the clinical pathological data of children with RB and found that the expression of SPRY2 and ESRRB is closely related to choroidal invasion, optic nerve invasion, and degree of differentiation. In the literature by Zhao *et al*[31], it was shown that miR-21 can target SPRY2 to promote the proliferation of epidermal growth factor-induced pancreatic cancer cells. In the studies by Yu *et al*[32] and Castet *et al*[33], it was shown that ESRRB can induce p21/CDKN1A to directly bind to the ERRE P21/CDKN1A promoter, thereby inhibiting the promotion of cell apoptosis and cell growth. However, we did not observe the biological functions of SPRY2 and ESRRB in RB cell lines in this study, which is a limitation of our research. The mechanism by which the differential expression of SPRY2 and ESRRB occurs in RB still needs further investigation. The specific regulatory mechanisms of SPRY2 and ESRRB in RB require further cell-based experiments (*e.g.*, gene knockout/overexpression). The results of this study provide preliminary evidence for their use as diagnostic markers.

CA199 is a common tumor marker in clinical practice, and its content in the serum of normal people is very low. It is mainly distributed in the gallbladder, pancreas, liver and intestines[34]. Previous studies have confirmed that CA199 is the most sensitive tumor marker in the diagnosis of pancreatic cancer[35]. In the study by Liu *et al*[14], the detection of tumor markers in the serum of RB patients before and after treatment revealed that CA199 has a more significant effect on the diagnosis and treatment of RB than other tumor markers. Therefore, we selected CA199 for correlation analysis with SPRY2 and ESRRB. The results showed that the expression of SPRY2 and ESRRB was negatively correlated with CA199, and the

difference was relatively significant. This indicates that there is a relationship between SPRY2, ESRRB and CA199. However, it is still unclear whether there is a regulatory relationship between the two, and whether the regulation is direct or indirect.

Based on the above research and relevant literature, we have preliminarily demonstrated the potential role of SPRY2 and ESRRB in RB. However, there are still some limitations in our study. First, we did not verify the effects of SPRY2 and ESRRB on the biological functions of RB cells *in vitro*. Second, we did not analyze the relationship between SPRY2, ESRRB and the survival of children. It is still unclear whether they can serve as potential prognostic markers for RB. Finally, we did not detect whether the expression of SPRY2 and ESRRB in the serum of patients changed after treatment. Therefore, we hope to increase clinical basic experiments and collect the overall survival time of patients in future studies to further analyze the value of SPRY2 and ESRRB in RB.

In summary, the expression of SPRY2 and ESRRB is closely related to the occurrence and development of RB and has the potential to be a diagnostic marker for RB and the universality of CA199 needs to be verified with a larger sample size.

ACKNOWLEDGEMENTS

Authors' Contributions: All authors significantly contributed to the manuscript revisions. Liu CY and Luo R contributed equally to this work. Liu CY and Luo R: experimental design, data interpretation, conceptualization, writing–original draft. Liu H and Xie RY: data collection, data interpretation. Chai Y and Xu Y: conception of the project, supervision, funding acquisition, writing–review & editing.

Data Availability: All data and materials are available in the article upon reasonable request to the corresponding authors.

Conflicts of Interest: Liu CY, None; **Luo R,** None; **Liu H,** None; **Xie RY,** None; **Chai Y,** None; **Xu Y,** None.

REFERENCES

1 Nag A, Khetan V. Retinoblastoma–a comprehensive review, update and recent advances. *Indian J Ophthalmol* 2024;72(6):778-788.

2 Wang L, Chen J, Shen Y, *et al*. Incidence, mortality, and global burden of retinoblastoma in 204 countries worldwide from 1990 to 2021: data and systematic analysis from the Global Burden of Disease Study 2021. *Neoplasia* 2025;60:101107.

3 Kaliki S, Taneja S, Palkonda VAR. Inadvertent intraocular surgery in children with unsuspected retinoblastoma: a study of 14 cases. *Retina* 2019;39(9):1794-1801.

4 Yang L, Shen JQ, Cheng YH. Expressions of p-STAT3, MMP-2 and VEGF in retinoblastoma. *Journal of Shandong University (Health Sciences)* 2009;47(5):113-116.

5 Sheu ML, Pan LY, Hu HY, *et al*. Potential therapeutic effects of thiazolidinedione on malignant glioma. *Int J Mol Sci* 2022;23(21): 13510.

6 Zhang Y, Wang Y, Zhi T, *et al*. Clinical characteristics, treatment and prognosis of infants with retinoblastoma: a multicenter, 10-year retrospective analysis. *BMC Pediatr* 2023;23(1):229.

7 Liu L, Zhong X, Zhong Y, *et al*. Recent advances in biomarker detection of oral squamous cell carcinoma. *Front Oncol* 2025;15:1597086.

8 Sayers EW, Beck J, Bolton EE, *et al*. Database resources of the national center for biotechnology information in 2025. *Nucleic Acids Res* 2025;53(D1):D20-D29.

9 Zhu Y, Wang Y, Hu M, *et al*. Identification of oncogenes and tumor-suppressor genes with hepatocellular carcinoma: a comprehensive analysis based on TCGA and GEO datasets. *Front Genet* 2022;13:934883.

10 Alameer A, Chicco D. geoCancerPrognosticDatasetsRetriever: a bioinformatics tool to easily identify cancer prognostic datasets on Gene Expression Omnibus (GEO). *Bioinformatics* 2022;38(6):1761-1763.

11 Zhao J, Xu Y, Gao Y, *et al*. A novel lncRNA MSTRG.16386.1 as ceRNA promotes kidney injury induced by deep hypothermic circulatory arrest *via* mediating miR-466b-5p/Spry2 axis. *FASEB J* 2026;40(1):e71342.

12 Ye J, Liu W, Yu X, *et al*. TRAF7-targeted HOXA5 acts as a tumor suppressor in prostate cancer progression and stemness *via* transcriptionally activating SPRY2 and regulating MEK/ERK signaling. *Cell Death Discov* 2023;9(1):378.

13 Sarin H. Molecular, pharmacologic and biochemical aspects of polycarbonate plastic bisphenol exposures. *Bisphenols-New Environmental, Pathophysiological and Social Perspectives*. London:IntechOpen; 2025.

14 Liu ZP, Zhou KY, Chen LL, *et al*. A preliminary study of retinoblastoma-related serum tumor markers. *Zhongguo Dang Dai Er Ke Za Zhi* 2017;19(3):318-321.

15 Li C, Zhang L, Zhang J, *et al*. Global, regional and national burden due to retinoblastoma in children aged younger than 10 years from 1990 to 2021. *BMC Med* 2024;22(1):604.

16 Alfaar AS, Halalsheh H, Shelil AE, *et al*. Nationwide incidence and survival of retinoblastoma in the USA between 1996 and 2018: a review of 5730 cases. *Ophthalmic Genet* 2025;46(2):144-153.

17 Wong ES, Choy RW, Zhang YZ, *et al*. Global retinoblastoma survival and globe preservation: a systematic review and Meta-analysis of associations with socioeconomic and health-care factors. *Lancet Glob Health* 2022;10(3):e380-e389.

18 Global Retinoblastoma Study Group. The Global Retinoblastoma Outcome Study: a prospective, cluster-based analysis of 4064 patients from 149 countries. *Lancet Glob Health* 2022;10(8):e1128-e1140.

19 Li GH, Peng YY. RNA interference technology's research progress in the treatment of retinal disease. *Guoji Yanke Zazhi (Int Eye Sci)* 2013;13(5):901-904.

20 Thangavelu PU, Lin CY, Forouz F, *et al*. The RB protein: more than a sentry of cell cycle entry. *Trends Mol Med* 2025;31(12):1124-1139.

21 Goodwin S, McPherson JD, McCombie WR. Coming of age: ten years of next-generation sequencing technologies. *Nat Rev Genet* 2016;17(6):333-351.

22 Tomczak K, Czerwińska P, Wiznerowicz M. The Cancer Genome Atlas (TCGA): an immeasurable source of knowledge. *Contemp Oncol (Pozn)* 2015;19(1A):A68-77.

23 Toro-Domínguez D, Martorell-Marugán J, López-Domínguez R, *et al*. ImaGEO: integrative gene expression meta-analysis from GEO database. *Bioinformatics* 2019;35(5):880-882.

24 Mao J, Lu M, Lu S, *et al*. Retinoblastoma gene expression profiling based on bioinformatics analysis. *BMC Med Genomics* 2023;16(1):101.

25 Zhang K, Fu R, Liu R, *et al*. Circulating cell-free DNA-based multi-cancer early detection. *Trends Cancer* 2024;10(2):161-174.

26 Panda SS, Sahoo RK, Patra SK, *et al*. Molecular insights to therapeutic in cancer: role of exosomes in tumor microenvironment, metastatic progression and drug resistance. *Drug Discov Today* 2024;29(8):104061.

27 Ma N, Li S, Zhang Q, *et al*. Long non-coding RNA GAS5 inhibits ovarian cancer cell proliferation *via* the control of microRNA-21 and SPRY2 expression. *Exp Ther Med* 2018;16(1):73-82.

28 Lao DH, Chandramouli S, Yusoff P, *et al*. A Src homology 3-binding sequence on the C terminus of Sprouty2 is necessary for inhibition of the Ras/ERK pathway downstream of fibroblast growth factor receptor stimulation. *J Biol Chem* 2006;281(40): 29993-30000.

29 Knudsen TE, Hamilton WB, Proks M, *et al*. A bipartite function of ESRRB can integrate signaling over time to balance self-renewal and differentiation. *Cell Syst* 2023;14(9):788-805.e8.

30 Mustafi D, Kevany BM, Genoud C, *et al*. Defective photoreceptor phagocytosis in a mouse model of enhanced S-cone syndrome causes progressive retinal degeneration. *FASEB J* 2011;25(9):3157-3176.

31 Zhao Q, Chen S, Zhu Z, *et al*. miR-21 promotes EGF-induced pancreatic cancer cell proliferation by targeting Spry2. *Cell Death Dis* 2018;9(12):1157.

32 Yu S, Wong YC, Wang XH, *et al*. Orphan nuclear receptor estrogen-related receptor-β suppresses *in vitro* and *in vivo* growth of prostate cancer cells *via* p21WAF1/CIP1 induction and as a potential therapeutic target in prostate cancer. *Oncogene* 2008;27(23):3313-3328.

33 Castet A, Herledan A, Bonnet S, *et al*. Receptor-interacting protein 140 differentially regulates estrogen receptor-related receptor transactivation depending on target genes. *Mol Endocrinol* 2006;20(5):1035-1047.

34 Meng M, Shi LL. Serum tumor markers expression (CA199, CA242, and CEA) and its clinical implications in type 2 diabetes mellitus. *World J Diabetes* 2024;15(2):232-239.

35 Staal B, Liu Y, Barnett D, *et al*. The sTRA plasma biomarker: blinded validation of improved accuracy over CA19-9 in pancreatic cancer diagnosis. *Clin Cancer Res* 2019;25(9):2745-2754.